

## Deploying solar photovoltaic energy first in carbon-intensive regions brings gigatons more carbon mitigations to 2060

Shi Chen<sup>1</sup>, Xi Lu<sup>1,2,3✉</sup>, Chris P. Nielsen<sup>4</sup>, Michael B. McElroy<sup>4,5✉</sup>, Gang He<sup>6</sup>, Shaohui Zhang<sup>7,8</sup>, Kebin He<sup>1,3</sup>, Xiu Yang<sup>9</sup>, Fang Zhang<sup>10</sup> & Jiming Hao<sup>1,3</sup>

The global surge in solar photovoltaic (PV) power has featured spatial specialization from manufacturing to installation along its industrial chain. Yet how to improve PV climate benefits are under-investigated. Here we explore the evolution of net greenhouse gas (GHG) mitigation of PV industry from 2009–2060 with a spatialized-dynamic life-cycle-analysis. Results suggest a net GHG mitigation of 1.29 Gt CO<sub>2</sub>-equivalent from 2009–2019, achieved by 1.97 Gt of mitigation from installation minus 0.68 Gt of emissions from manufacturing. The highest net GHG mitigation among future manufacturing-installation-scenarios to meet 40% global power demand in 2060 is as high as 204.7 Gt from 2020–2060, featuring manufacturing concentrated in Europe and North America and prioritized PV installations in carbon-intensive nations. This represents 97.5 Gt more net mitigation than the worst-case scenario, equivalent to 1.9 times 2020 global GHG emissions. The results call for strategic international coordination of PV industrial chain to increase GHG net mitigation.

<sup>1</sup>School of Environment, State Key Joint Laboratory of Environment Simulation and Pollution Control, Tsinghua University, Beijing, China. <sup>2</sup>Beijing Laboratory of Environmental Frontier Technologies, Tsinghua University, Beijing 100084, China. <sup>3</sup>Institute for Carbon Neutrality, Tsinghua University, Beijing, China. <sup>4</sup>Harvard-China Project on Energy, Economy and Environment, Harvard John A. Paulson School of Engineering and Applied Sciences, Harvard University, Cambridge, USA. <sup>5</sup>Department of Earth and Planetary Sciences, Harvard University, Cambridge, USA. <sup>6</sup>Marx School of Public and International Affairs, Baruch College, City University of New York, New York, USA. <sup>7</sup>School of Economics & Management, Beihang University, Beijing, China. <sup>8</sup>International Institute for Applied Systems Analysis (IIASA), Laxenburg, Austria. <sup>9</sup>The Institute of Climate Change and Sustainable Development, Tsinghua University, Beijing, China. <sup>10</sup>School of Public Policy & Management, Tsinghua University, Beijing, China. ✉email: [xilu@tsinghua.edu.cn](mailto:xilu@tsinghua.edu.cn); [mbm@seas.harvard.edu](mailto:mbm@seas.harvard.edu)

To achieve a global target of net-zero carbon emissions by 2050 requires substantial scaling up of solar photovoltaic (PV) and other renewable energy production<sup>1–3</sup>. The global installed capacity of solar PV power has increased 30-fold from 2009 to 2019, while its cost of generation has declined by 90%<sup>4</sup>. In the global transition towards carbon neutrality pledged by 137 nations to date<sup>5</sup>, solar PV is expected to play a critical role, with the worldwide installed capacity projected to meet more than 30% of power demand by 2050<sup>6,7</sup>. Given disparate national development trajectories within the global evolution of the entire PV industrial chain from manufacturing to installation, the spatial differences and temporal dynamics of GHGs both emitted throughout PV production and mitigated through its displacement of thermal power are critical to successful achievement of global zero-emission scenarios. Failure to consider these factors, which are currently under analyzed in the scientific literature, risks missing opportunities in the global PV deployment trajectory to maximize net life-cycle GHG mitigation of solar power.

The solar PV industrial chain, from manufacturing to installation, and future disposal and recycle, has become increasingly specialized by national policies and international trade. The historical deployment patterns of manufacturing facilities and installed solar power capacity have been largely driven by industrial competitiveness and national climate ambitions; the global hotspots for growth of installed capacity have been shifting recently from Europe to the Asia-Pacific<sup>8</sup>. Europe led global installed solar PV capacity until 2016, when its cumulative capacity of 104.6 GW was overtaken by that of the Asia-Pacific, with 145.9 GW<sup>9</sup>. The Asia-Pacific share of global installed capacity surged to 52% in 2019, with China alone accounting for 32.9%<sup>8</sup>. Along with the change in geographical distribution of installed capacity, the manufacturing of products from polysilicon to wafers, cells and modules has also undergone a dynamic spatial shift, becoming gradually concentrated in the Asia-Pacific<sup>10</sup>. This evolution of the global solar PV industrial chain directly shapes the spatial and temporal distributions of its net effects on GHG mitigation.

Furthermore, there have been simultaneous appeals in recent years to reorient solar PV manufacturing to increase regional and national resilience of solar PV supply. It is estimated that the world will rely almost completely on China to produce key components of solar panels by 2025, driving widespread calls for diversification of the PV manufacturing supply chain within the international community<sup>11</sup>. Since 2020, countries have increasingly enacted policies to encourage domestic production of solar PV products. Since 2021, the United States has reaffirmed goals of increased resilience of clean energy supply in its economic stimulus package and the Inflation Reduction Act<sup>12</sup>. The spatial and temporal differences in industry chain emissions are thus affected by the potential solar PV manufacturing shifts under international net-zero objectives and disparities in emissions intensities among manufacturers.

In the context of both a global surge in installations and accelerated international specialization and changes in the industry, it is imperative to understand the impact of the patterns of global PV industrial chain deployment on net GHG mitigation, including its spatiotemporal determinants. A large body of literature has utilized methods of life cycle assessment (LCA) and conventional emission inventories to examine location-specific GHG emissions or mitigation attributable to PV deployment in China<sup>13–20</sup> and worldwide<sup>21–23</sup>. However, the study of emissions and mitigation have not sufficiently characterized the spatiotemporal evolution of both the intensities of GHG emissions and mitigation per unit of solar PV manufactured and installed<sup>24</sup>, which are influenced by factors along the entire industrial chain that include technical and energy use efficiency, solar resource

availability and consequent power generation, and the average emissions of the local power system providing electricity to PV production. Furthermore, such differences are inadequately accounted for in projections given the multiple uncertainties concerning patterns of industrial chain deployment. This may not only lead to bias in total accounting but is also insufficient to support cross-country comparisons and optimization of deployment strategies. Spatiotemporal analyses with improved timelines and resolution will become increasingly valuable for maximizing GHG mitigation from solar PV deployment, especially in the increasingly complex global industrial chain forged in the last half decade and projected into the future<sup>25</sup>.

The aim of this analysis is to quantify in spatiotemporal terms the net GHG mitigation of the global solar PV industrial chain for the periods 2009–2019 and 2020–2060, using a LCA model considering dynamics of spatial parameters that evolve interdependently under multiple industrial chain patterns (Fig. 1). Results suggest that the cumulative global emissions and mitigation of GHGs by 2019 were respectively 680.3 and 1968.8 Mt of CO<sub>2</sub>-equivalent (CO<sub>2</sub>e), of which 66.1% and 35.8% were attributable to China's PV industry. Nine scenarios based on combinations of possible manufacturing (M1–M3) and installation (C1–C3) patterns (Table 1) are employed to evaluate the net GHG mitigation from PV production and deployment by 2060. At the low end is 107.2 Gt CO<sub>2</sub>e of net mitigation, resulting from 116.1 Gt mitigation from PV installations following their current geographical distribution, offset by 8.9 Gt emissions from manufacturing concentrated in the Asia-Pacific (scenarios C1–M2). At the high end is 204.7 Gt, resulting from 209.3 Gt of emissions mitigation from installations targeted for the objective and offset by 4.6 Gt emissions from manufacturing in the Europe and North America (scenarios C3–M3). The increase in net mitigation from C1–M2 to C3–M3 is equivalent to 1.9 times global GHG emissions in 2020. Such an increase requires a spatial shift of newly installed capacity to the Middle East, Southeast Asia, and Eurasia. To our knowledge, the study is the first to systematically account for historical and future emissions and mitigation of GHGs from solar PV deployment globally. The results can inform cooperative international strategies to develop the solar PV industry to speed the transition towards global carbon neutrality.

## Results

**Spatiotemporal characteristics of net GHG mitigation from historical PV manufacturing and installation.** Annual emissions and mitigation of GHGs of the entire solar PV power industrial chain are quantified at the country level from 2009 to 2019, based on activity levels of all relevant processes from manufacturing of metallurgical silicon to solar power generation and the spatiotemporal GHG emission and mitigation intensities of both monocrystalline silicon and polysilicon technologies. Net GHG mitigation, defined as the difference between mitigation and emissions of GHGs, is used to characterize the life-cycle GHG mitigation performance of solar PV power across nations (Fig. 2a). The global cumulative net GHG mitigation from 2009 to 2019 is estimated at 1288.5 Mt CO<sub>2</sub>e, equal to 0.36% of global CO<sub>2</sub> emissions during the same period. This global net mitigation is achieved through GHG mitigation of 1968.8 Mt CO<sub>2</sub>e, offset partially by GHG emissions from PV production and deployment of 680.3 Mt CO<sub>2</sub>e (Supplementary Figure 1). As indicated in Fig. 2a, the cumulative amounts of net mitigation in the Asia-Pacific, Europe and North America accounted for 51.5%, 29.8% and 13.4% of global total respectively (see Supplementary Table 1 for the aggregation of the countries by region). The net GHG mitigation of solar PV in other regions accounted for only 5.3% of the global total, including 2.5% from Africa, 1.4% from the

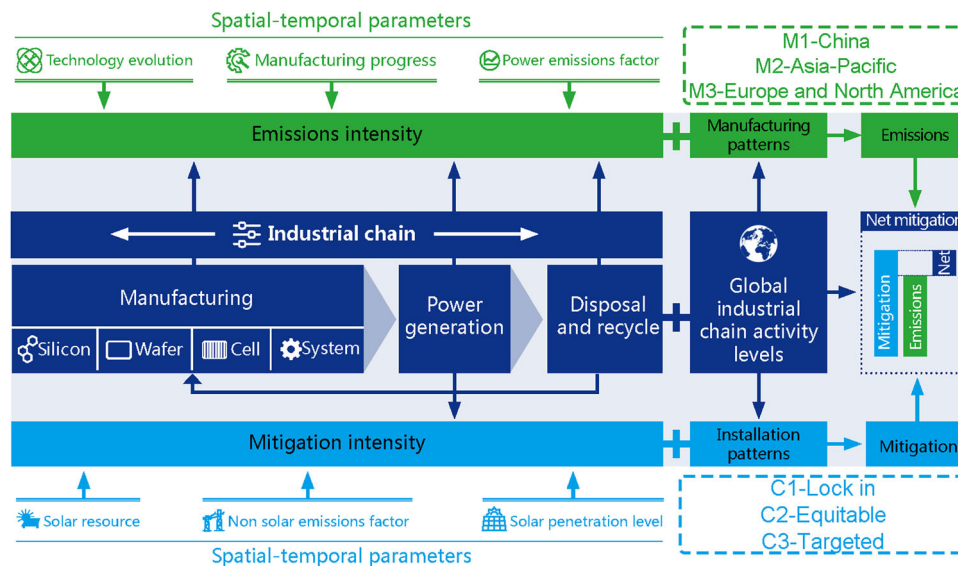


**Fig. 1 A spatial-temporal life-cycle-assessment model to quantify the global greenhouse gases (GHG) emissions and mitigation of solar PV industrial chain.** Annual GHG emissions and mitigation of the entire solar PV power industrial chain are quantified at the country level, based on the spatiotemporal GHG emission and mitigation intensities, and activity levels of all relevant processes from production of metallurgical-grade silicon to the recycle of the solar PV power generation system. In addition to historical accounting, the study quantifies how GHG emissions and mitigation evolve under different industrial chain development patterns, through combining global differences in projective emission and mitigation intensities with 3 manufacturing patterns (M1-M3) and 3 installation patterns (C1-C3).

Middle East and 1.3% from Central and South America. Countries including South Korea, Malaysia and Singapore who are PV manufacturers but comparatively minimal PV installers had negative net cumulative GHG mitigation by end of 2019, with a total of  $-42.4$  Mt. The top 5 countries, China, Japan, the United States (US), Germany and India achieved the highest cumulative net GHG mitigation at 266.3, 198.2, 167.9, 157.3, and 144.0 Mt respectively, together accounting for 72.5% of the global total (Supplementary Figure 2). These countries are large PV installers, with 71.4% of worldwide capacities collectively in 2019. The top five countries in net mitigation were also PV manufacturing powerhouses, accounting for 82.3% of cumulative emissions from 2009 to 2019.

Temporally, annual net GHG mitigation increased quickly as installed capacity grew and resulting mitigated emissions surpassed those produced during PV manufacturing. Thanks to rapid expansion of domestic solar PV installations after initially producing mainly for export markets<sup>25</sup>, net mitigation in China became positive in 2017 and constituted the largest share of annual global net mitigation in 2019, accounting for 20.6% of the total. China's share of manufactured products from polysilicon to silicon wafers, PV cells, and modules increased from 19%, 73%, 44% and 43% in 2009 to 68%, 96%, 79% and 71% of the global totals in 2019, respectively<sup>8</sup>. Due to expansion of global demand and agglomeration of production along the industrial chain in China, emissions from manufacturing processes did increase 17.6 times in the same period, however the ratio of emissions to mitigation decreased from a factor of 48 in 2009 to just 0.286 in 2019 (Fig. 2b). As earlier adopters of solar PV before China, net GHG mitigation in Germany, Japan and the US became positive in 2010, 2011 and 2014 respectively. However, the share of global net mitigation from Germany and Japan declined from 41.0% and 25.7% in 2015 to 12.2% and 15.4% in 2019, and the US increased the share modestly from 12.8% to 13.0% during the same period, mainly due to their rates of increased GHG mitigation lagging far behind those of emerging economies like China and India (Fig. 2b). India increased its share of global net GHG mitigation through PV deployment from 0.4% to 7.4% during 2015 to 2019,

due to growing installed capacity offset only slightly by emissions associated with emerging PV manufacturing.

**Spatiotemporal variation of mitigation and emissions intensities.** Global GHG mitigation and emissions from solar PV power are driven not only by its expanding scale, but also by the varied spatial and temporal dynamics of mitigation and emissions intensities of the links of its industrial chain. The achievable GHG mitigation is dependent on the scale and pace of solar PV deployment, as well as the GHG mitigation intensity. The mitigation intensity, characterized by annual GHG mitigation or avoided emissions per kW installation (in  $\text{kg CO}_2\text{e kW}^{-1} \text{a}^{-1}$ ), is determined by the solar resource availability and the emissions factor of the replaced energy source, assumed here to be electricity from national power grid<sup>26</sup>. The theoretical GHG mitigation intensity shows spatial differences and temporal variations due to the differences in solar resource availability, and the emission factors of national power systems (Fig. 3a, b). Spatially, the theoretical GHG mitigation intensity, averaged from 2009 to 2019, was highest for the Middle East at  $1293.9 \text{ kg CO}_2\text{e kW}^{-1} \text{a}^{-1}$ ; this is due to a combination of strong solar resources and high average emission factors for the power grid. Africa and the Asia-Pacific rank next in levels of mitigation intensities, at 889.2 and  $803.9 \text{ kg CO}_2\text{e kW}^{-1} \text{a}^{-1}$  respectively. Theoretical GHG mitigation intensity was lowest for Eurasia, North America, Central and South America, and Europe, averaging  $586.3 \text{ kg CO}_2\text{e kW}^{-1} \text{a}^{-1}$ . Such differences reflect those advanced economies can only realize lower marginal GHG mitigation when installing solar PV, compared to developing economies. Consequently, in regions where the electrification rate is low, like sub-Saharan Africa, the theoretical GHG mitigation potential of solar PV could be even higher if directly substituting instead for biomass combustion, which normally yields higher GHG emissions compared to electricity generation<sup>27,28</sup>. If the spatial differences in mitigation intensities are ignored and the lowest or highest national mitigation intensities applied worldwide, estimates of historical mitigation would be subject to errors of  $-7.9\%$  or  $15.1\%$  respectively (Supplementary Figure 3).

**Table 1 Scenarios of national distributions of new manufacturing and new installations of solar PV.**

Manufacture		M1 - China	M2 - Asia-Pacific	M3 - Europe and North America
<b>Shared assumption</b>	New distributions are established by 2030 and they are held constant at 2030 levels.	90% of production in each process will be concentrated in China by 2030 following recent trends, with the remaining 10% distributed according to the current (2019) national shares.	90% of production will relocate to Asian-Pacific countries other than China by 2030, taking advantage of low manufacturing costs and a relatively open international trade environment. Remaining 10% as per MI.	90% of production will relocate to the 2019 top 5 installing nations in the European Union and North America by 2030, in accordance with strategies to enhance self-sufficiency. Remaining 10% as per M2.
Installation		C1 - Lock in	C2 - Equitable	C3 - Targeted
<b>Shared assumption</b>	Solar PV capacity is set to meet 30% and 40% of global power demand by 2050 and 2060	New solar installations will lock in the current pattern, the higher the current (2019) solar share meeting its power demand, the higher new solar installations share in each nation's future power demand.	New solar installations will be balanced across nations so that they will serve the same shares of power consumption of all nations.	New solar installations will be prioritized for countries with the highest emission factors for their power systems.

The global average theoretical GHG mitigation intensity of solar PV has declined 11.1% from 2009 to 2019 (Fig. 3b). The GHG mitigation intensity for China fell by 22.3%, from 1261.3 kg CO<sub>2</sub>e kW<sup>-1</sup> a<sup>-1</sup> in 2009 to 980.4 kg CO<sub>2</sub>e kW<sup>-1</sup> a<sup>-1</sup> in 2019, driven by the combustion efficiency retrofits of coal-fired power plants as well as the large-scale deployment of renewable power sources<sup>29,30</sup>. Such declines in Europe and North America have been larger, with 75%, 49%, 32%, and 27% declines respectively for Denmark, Finland, Italy, and Germany, and 27% and 25% declines for the US and Canada. Regionally, the 24.9% decline in Europe is the most substantial, where the electricity sector has already undergone rapid decarbonization<sup>31</sup>. In contrast, the decline in theoretical GHG mitigation intensity has been much lower for Africa and Eurasia regions, at 5.4% and -3.7% during the same period, where low-carbon transformations of power systems have progressed slowly on average, or not at all<sup>32</sup>. As a result, the theoretical GHG mitigation intensity for Africa in 2019 is 2.0 times that of Europe. As indicated in Fig. 3b, theoretical GHG mitigation intensities from PV deployment increased for African and Eurasian countries like Mozambique, Zambia, Togo, and Armenia from 2009 to 2019, which spotlights not only the need to decarbonize their power sectors, but also an opportunity to accelerate such progress given the abundance of their geophysical solar resources. If the temporal dynamics of the mitigation intensities were not taken into consideration and the static mitigation intensities of 2009 or 2019 had been applied throughout the period, the global mitigation would have been overestimated by 26.7% or underestimated by 27.0%, accordingly (Supplementary Figure 3).

The theoretical GHG emission intensity for each country, expressed as the aggregate GHG emissions resulting from the manufacturing and power generation of a functional unit of solar PV, defined here as a 1kW power generation system, are summarized for 2009 and 2019 in Fig. 4a, b (with the system boundary and sequential steps in the industrial chain in Supplementary Figure 4). All steps in manufacturing are categorized into four sequential processes including solar-grade silicon, wafer, cell, and system to facilitate the interpretation of the results (including module and other components of the system other than module, or balance of system). The GHG emission intensity shows clear spatial disparities among nations, especially in the earlier year of 2009. The theoretical life cycle GHG emission intensities in 2009 for countries participating in manufacturing range from 3875.3 kg CO<sub>2</sub>e kW<sup>-1</sup> for India to 1189.5 kg CO<sub>2</sub>e kW<sup>-1</sup> for Canada, due largely to differences in the electric power capacity mix and resulting emission factors. By 2019, the gap between high and low theoretical GHG emission intensities narrows by 82.5%, to 471.3 kg CO<sub>2</sub>e kW<sup>-1</sup> (Fig. 4b; see year-to-year variations of the emission intensities for the manufacturing processes for solar-grade silicon, wafer, cell, and system for PV monocrystalline and polysilicon systems from 2009 to 2019 in Supplementary Figure 5).

Temporally, as indicated in Fig. 4b, the theoretical global average GHG emission intensity of solar PV power for the functional unit declined by 74.7% from 2009 to 2019 (Supplementary Table 2-3). The GHG emission intensity declined by 2859.5 kg CO<sub>2</sub>e kW<sup>-1</sup>, or 79.2%, in China, whose market share in each manufacturing process was 70% or higher in 2019. The year-to-year variations in emissions intensities associated with manufacturing processes (Supplementary Figure 5) are composite effects from both the resource efficiency in the manufacturing process and with changing emission factors of energy consumed, and advancements in technical parameters. Taking China as an example, the decrease in GHG emission intensity of China's PV full industry chain is attributed to direct reductions of electricity consumption and silicon consumption in production, an increase

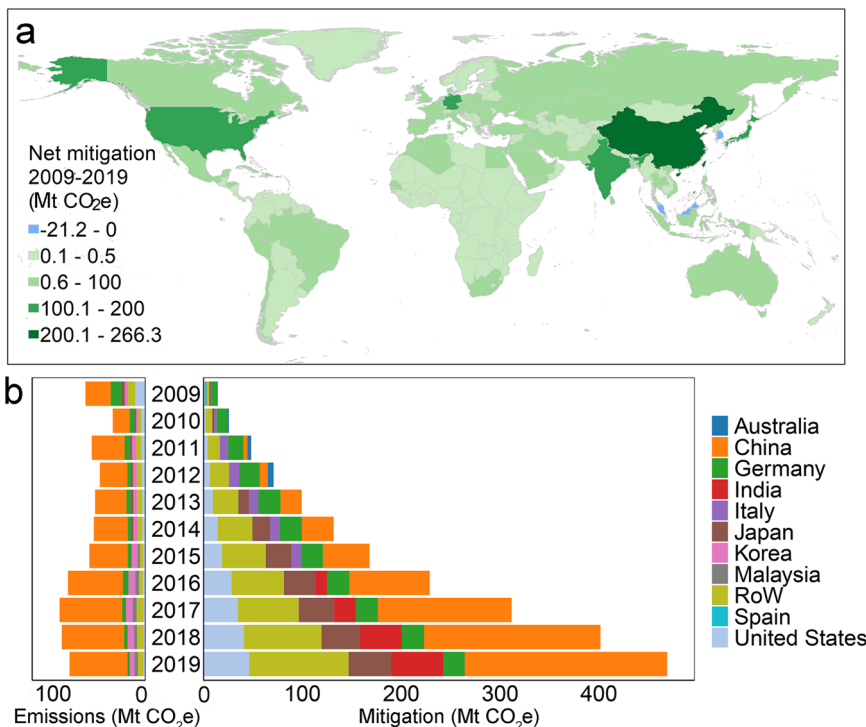


**Fig. 2 Spatial imbalance in global net GHG mitigation from solar PV power during 2009-2019. a** Spatial distribution of cumulative net GHG mitigation, defined as the difference between mitigation and emissions of GHGs. **b** Historical annual global GHG emissions and mitigation. Colors suggest contributions from the top 5 countries each year and rest of world (RoW).

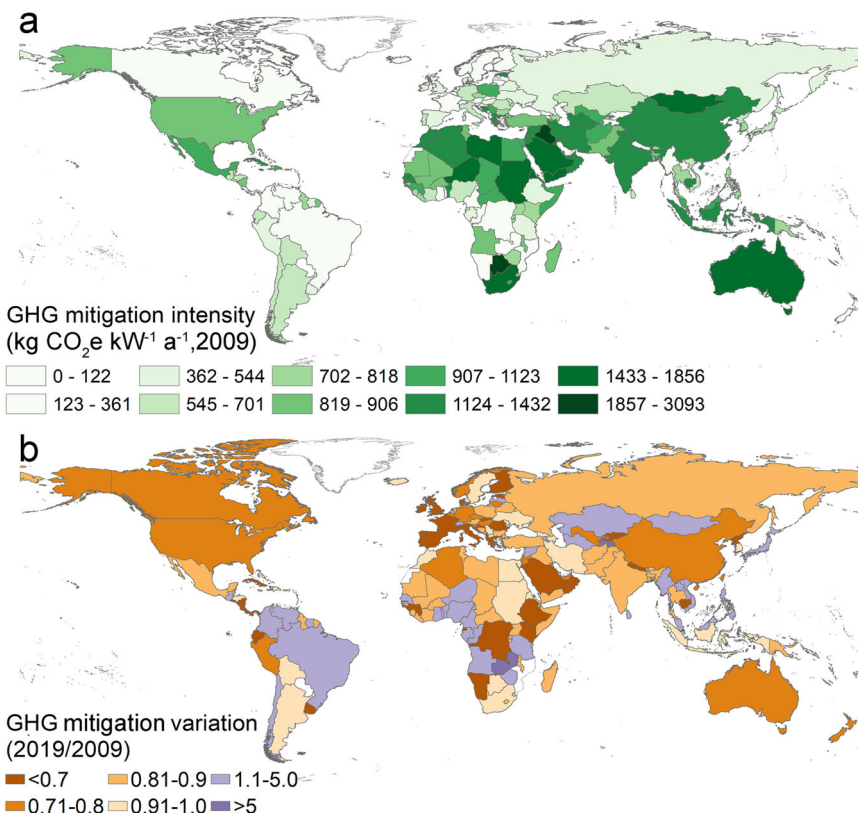


**Fig. 3 Spatial disparity and temporal dynamics of theoretical GHG mitigation intensity from solar PV power. a** GHG mitigation intensity per unit installed solar power in 2009. **b** The variation of GHG mitigation intensity expressed as the ratio of mitigation intensity in 2019 to that of 2009.

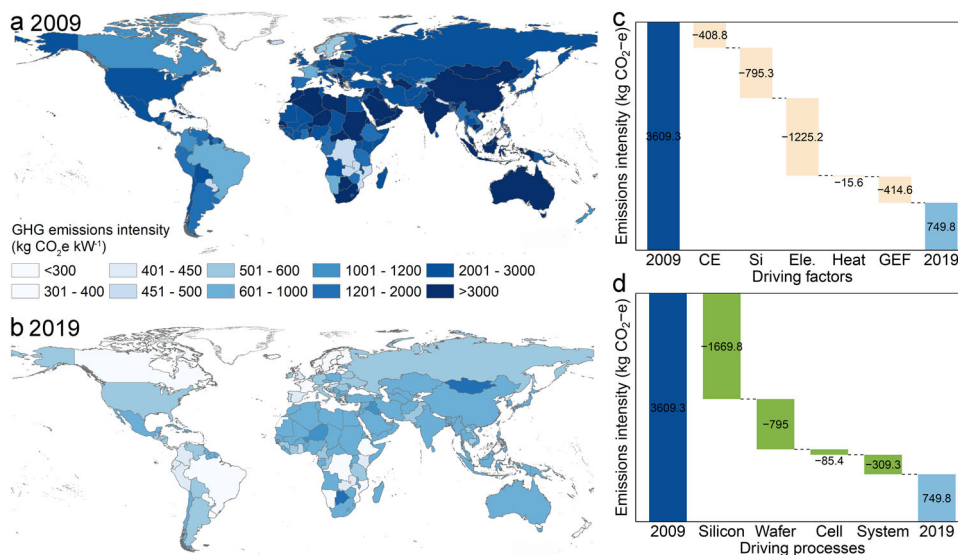


**Fig. 4 Spatial disparity and temporal dynamics of theoretical GHG emission intensity from solar PV power, expressed in kg CO<sub>2</sub>e per kW.** **a** Theoretical GHG emission intensity of a functional unit of monocrystalline silicon PV in 2009. **b** The same as (a) but for 2019. The driving factors (c) and processes (d) associated with production of intermediate and final products for the decline in GHG emission intensity for China from 2009 to 2019. CE represents the impact of improvement of conversion efficiency; Si, Ele., and Heat represent the impact of declines in consumption of silicon, electricity, and heat; GEF represents the impact of the decline in average emission factors for grid power. The figure shows GHG emissions from production of metallurgical grade silicon to the active phase of the solar PV power generation system. The emissions during disposal and recycling processes, and the associated reduction of GHG emissions from using recycled materials during manufacturing, were not considered here because the disposal and recycling of systems were uncommon in these early years of the industry. Such processes are considered in the future projections discussed in the next section.

in solar-to-power conversion efficiency, and declines in the power generation emission factor and heat consumption by  $-42.8\%$ ,  $-27.8\%$ ,  $-14.3\%$ ,  $-14.5\%$  and  $-0.5\%$  respectively (Fig. 4c and Supplementary Figure 5). In terms of the processes associated with sequential steps in the industrial chain, the polysilicon, wafer, cell, and system contributed 58.4%, 27.8%, 3.0%, and 10.8% shares of the decline in total GHG emission intensity (Fig. 4d and Supplementary Figure 5). Much like the need to spatialize and temporalize GHG mitigation intensities when accounting for mitigation, spatial and temporal characteristics of GHG emissions intensities are also critical to the estimation of emissions; failing to do so could result in deviations up to  $-35.0\%$  to  $161.9\%$  in estimates of cumulative global emissions (Supplementary Figure 3). The existing research results exhibit a wide range of variations and relatively limited comparability<sup>33</sup>, attributed to different assumptions over multiple factors, such as system boundary, insolation, performance ratio, solar module efficiency, operating lifetime, type of installation, and geographical locations<sup>34</sup>. Our estimations complement existing numerous retrospective PV life-cycle studies by including temporal dynamics for countries worldwide under the same analytical framework (Supplementary Table 4). Moreover, the results for recent years indicate a decline in emissions, falling towards the lower end of the range in literature (Supplementary Table 4). The variation observed in our emissions estimation can be attributed to the integration of technological advancements and improvements in the emissions factor of the power grid in recent years.

#### Spatiotemporal variation of future mitigation and emissions.

According to the International Energy Agency (IEA), the global installed solar PV capacity is expected to meet 40% of power demand by 2060 in order to align with net-zero climate goals<sup>7</sup> (see Supplementary Figure 6 and Supplementary Table 5 for future power demand and solar power capacity projections with reference to leading models and projections); the magnitude and distribution of GHG emissions and mitigation will be increasingly

influenced by installation-manufacturing deployment strategies and the evolution of both emission and mitigation intensities. Here we project the GHG emissions and mitigation of the global industrial chain of solar PV power through three manufacturing scenarios (continued concentration in China, M1; transfer to other Asia-Pacific countries, M2; and transfer to the EU and North America, M3) combined with three PV power capacity installation scenarios until 2060 (locked-in current installation patterns, C1; equitable installation across countries, C2; and preferential installation in nations with emission-intensive thermal power systems, C3) (Table 1, see more detailed settings and assumptions in Methods and the regional distributions in Supplementary Figure 6 and Supplementary Table 6-8). The model limits PV generation to meet a maximum of 70% of national electricity demand while also not exceeding its theoretical geophysical potential for each nation<sup>35,36</sup>. Three scenarios of evolution of emission factors for non-solar power sources (conservative, moderate, and optimistic) are combined with the manufacturing-installation scenarios to evaluate the impact of the different decarbonization rates of non-solar power sources in each nation (See Supplementary Table 7). The study assumes the average life-cycle service time of a PV system is 25 years<sup>37</sup> and the newly-added capacity in each year will be provided first by manufacturing using recycled materials to the extent they are available, with the rest using new material inputs.

From an installation perspective, the deployment pattern of solar power is vitally important to exploiting its GHG mitigation potential. Expanded solar installations will allow greater substitution for thermal power generation, reducing the emission factor of the power system. And the GHG mitigation is defined as the power system emissions avoided of solar substitution compared to a base scenario where the solar installed capacity remains at the 2019 level and other assumptions remain the same. Cumulative mitigation of GHGs could reach 116.1 Gt of CO<sub>2</sub>e (86.5 Gt, 145.8 Gt) through scaling up capacity under an installation pattern locking in current national distributions (C1)

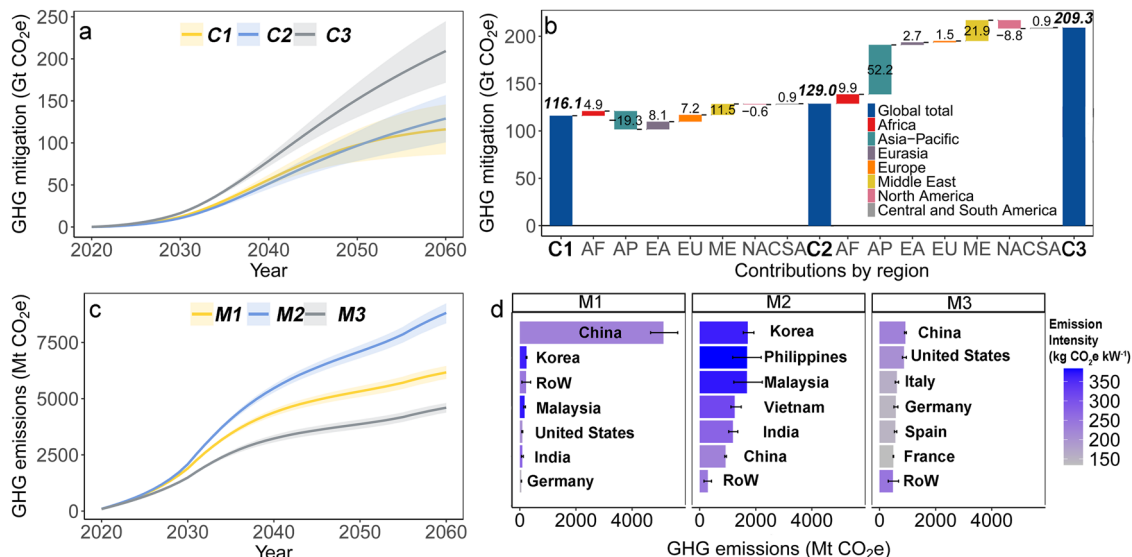


**Fig. 5 Future GHG mitigation and emissions of PV industry by scenario from 2020 to 2060.** **a** Cumulative global GHG mitigation under varied installation scenarios. The ribbon of light shading reflects the uncertainty under multiple scenarios of emission factors of non-solar power generation in each country and different solar PV installation scenarios. **b** Regional contributors to global GHG mitigation as it increases between C1, C2 and C3 scenarios. Panel **(c)** is similar to **(a)** but presents GHG emissions under varied manufacturing scenarios. **(B)** Regional contributors to global GHG mitigation as it increases between C1, C2 and C3 scenarios. **d** Contributions to GHG emissions of the leading emitting countries under M1-M3 manufacturing scenarios. The color indicates the average GHG emission intensities of manufacturing one functional unit from 2020 to 2060, including end-of-service disposal and recycling processes. The error bars reflect the uncertainties in GHG emissions influenced by scenarios of power grid emission factors and installation patterns.

(Fig. 5a) and increase to 129.0 Gt (100.7 Gt, 156.6 Gt) if capacity is scaled up on an equitable basis (C2). (Values in parentheses represent the range of mitigation uncertainties under different grid emission factor scenarios; values below without parenthetical ranges indicate the average of all scenarios.) Although the 12.9 Gt increase of GHG mitigation from C1 to C2 is modest, the regional difference in mitigation is notable and may be important for international carbon accounting (Fig. 5b). Compared to C1, the GHG mitigation in the Middle East, Eurasia, and Europe increases respectively by 11.5, 8.1 and 7.2 Gt under C2. The main contributors to the increase include Russia, Saudi Arabia, Iran, the United Arab Emirates (UAE) and Poland, all of which are relatively late deployers of solar PV (Supplementary Figure 7). In contrast, mitigation in the Asia-Pacific decreases by 19.3 Gt in the C2 scenario because of a decline in China that is only partially offset by increases in Indonesia, South Korea, and Malaysia (Supplementary Figure 7). If the pattern is further tailored to exploit comparative advantages in GHG mitigation intensities among nations (C3), the global GHG mitigation would further increase to 209.3 Gt (171.7 Gt, 244.7 Gt), of which the Asia-Pacific, Middle East and Africa contribute 55.2, 21.9 and 10.0 Gt of the increase, contributed mainly by India, Indonesia, Russia, Saudi Arabia, Iran, and UAE (Supplementary Figure 7). The solar PV installation shares of Africa, Eurasia, the Middle East, and Association of Southeast Asian Nations (ASEAN) regions in global installed capacity in 2060 would increase from 2.6%, 0.3%, 2.1 % and 1.6% under C1 to 8.9 %, 7.7 %, 9.4 % and 9.7% under C3. Average power grid emission factors from 2020 to 2060 for the top 10 countries in the C3 scenarios are 49.0% and 11.3% higher than those of the C1 and C2 scenarios, with India projected to have the highest GHG mitigation under C3.

The cumulative GHG emissions are lowest under the M3 manufacturing scenario at 4.6 Gt (4.4 Gt, 4.8 Gt), followed by M1 and M2 scenarios at 6.2 Gt (5.9 Gt, 6.5 Gt) and 8.9 Gt (8.4 Gt, 9.2 Gt) respectively (Fig. 5c), with results depending mostly on the manufacturing pattern but also influenced by the GHG emission

**Table 2 Projections of the GHG industry chain emissions intensity (g CO<sub>2</sub>e kWh<sup>-1</sup>) under multi-manufacturing-installation scenarios in 2030.**

Manufacture scenarios	Installation scenarios			
		C1	C2	C3
M1	China	7.5–15.1	8.2–16.4	7.7–15.4
	Korea	10.4–20.7	9.4–18.7	8.9–17.9
M2	India	9.1–18.2	9.9–19.8	8.1–16.2
	Malaysia	12.1–24.2	10.9–21.7	8.6–17.1
	Philippines	12.6–25.1	11.6–23.2	8.7–17.4
	Vietnam	8.3–16.6	9.1–18.2	8.7–17.5
M3	Canada	5.4–10.7	5–10	5.4–10.7
	United States	6.6–13.1	6.6–13.2	7.2–14.4
	Italy	5.6–11.2	5.3–10.5	5.6–11.2
	France	4–8	3.9–7.9	4–8
	Spain	4.8–9.6	4.8–9.6	5–10.1

(The ranges represent the emissions variation when utilization hours of solar PV varying from 1000 to 2000 h).

intensity. (Values in parentheses represent the range of emission uncertainties under different grid emission factor and solar installation scenarios; values below without parenthetical ranges indicate the average of all scenarios.) The results suggest that global GHG emissions could be substantially reduced through further industry agglomeration in countries with lower GHG emissions intensities in their industrial chains. From the perspective of the emissions per kWh electricity generated, the study projects a life-cycle CO<sub>2</sub> emissions in 2030 at 3.9–25.1 g CO<sub>2</sub>e kWh<sup>-1</sup>, with the difference depending mainly on manufacturing scenarios (Table 2). This implies that solar PV generates negligible GHG emissions compared to currently reported fossil fuel-based energy sources such as natural gas and coal, and even compared to most other low-carbon

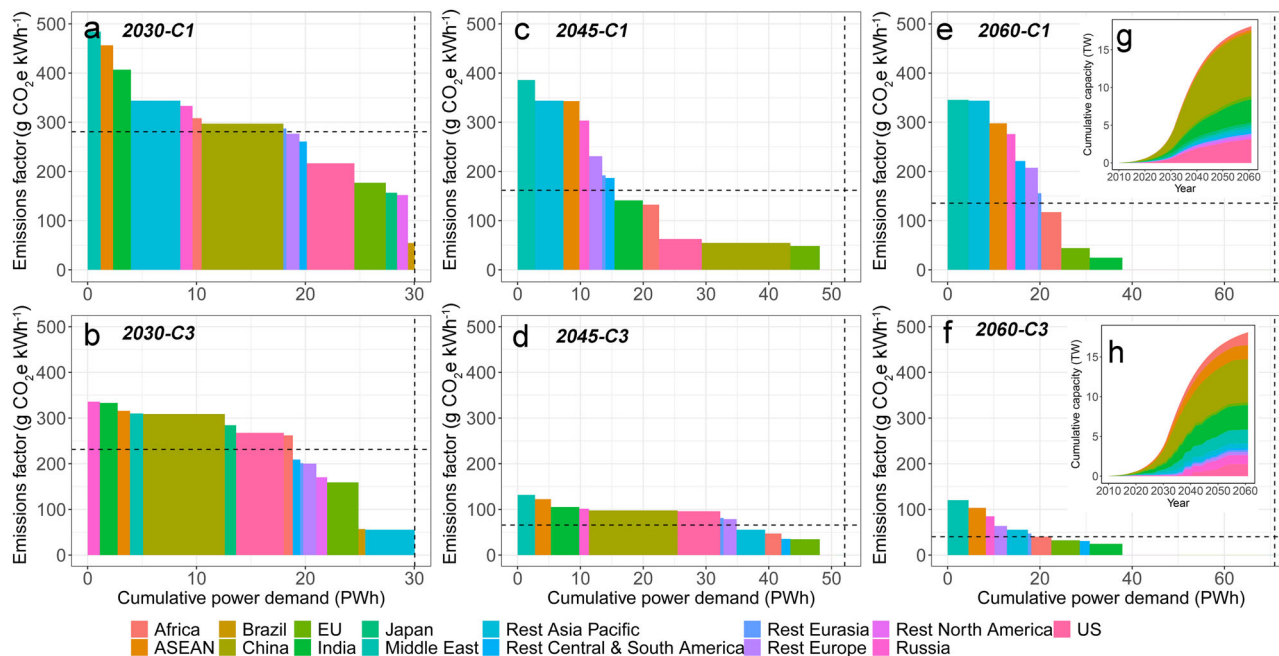


**Fig. 6** The impact of deployment strategies of the PV industry on the emission factors of national or regional power systems in 2030, 2045 and 2060.

**a** The relationship of power system emission factors and power demand under C1 in 2030 under a moderate rate of decline in the emission factor of non-solar power sources. The horizontal dashed line represents the global average emission factor. The vertical dashed line represents the projection of global electricity demand; note that no regional or national power system is fully decarbonized in 2030. The areas of the colored bars in each panel from **a–f** are proportional to the total emissions from the power systems. **b** The same as (**a**) but for C3, with installations targeted to countries with emission-intensive power systems. **c** The same as (**a**) but for 2045. **d** The same as (**c**) but for C3. **e** The same as (**a**) but for 2060. **f** The same as (**e**) but for C3. **g** Spatial distribution of cumulative installed capacity under C1. **h** The same as (**g**) but for C3.

technologies<sup>38</sup> (see Supplementary Table 9). CO<sub>2</sub> emissions under M2 scenario is 24.7% and 85% higher than M1 and M3 respectively. The emissions of the leading emitting nations under each manufacturing scenario are summarized in Fig. 5d. Under M1, China alone contributes 85.7% of global emissions. China also topped the cumulative emissions under M3, resulting mainly from its manufacturing processes with relatively higher emission intensities despite being partially offset by decreasing market share. Projections of global GHG emissions under M2 are highest among all manufacturing scenarios because of higher GHG emission intensities for manufacturing in Asia-Pacific countries. The average cumulative transportation emissions (including international and domestic transportation) among all scenarios until 2060 are estimated to be 0.45 Gt (Supplementary Methods and Tables 10–11). Here we assume in the base case that the end-of-life treatment of the PV system after commitment will evolve from landfill-dominant to recycling-dominant. The recycling rate will increase from 10% in 2020 to 100% in 2045, with a compound annual growth rate of 10%. Increased recycling will help greatly reduce GHG emissions from the industrial chain. Compared to a scenario where solar PV ends up in landfill only in all future years, the GHG emissions will be increased by 5.3–13.8% (Supplementary Table 12). This suggests that early recycling action could reduce GHG emissions in the future industrial chain.

Figure 6 shows the impact of the solar PV installation pattern on the power system emission factors and emissions (taking C1 and C3 under moderate reductions in non-solar emission intensities as examples). C3 decreases the global average emission factor of the power grid compared to C1 and reduces national differences (Fig. 6a–f). It is projected that by 2030, under C3, global average emission factors would be reduced by 17.6% compared to C1. The difference in global average emission factors

between C3 and C1 would be further increased to 59.3% and 70.4% in 2045 and 2060. Additionally, the global spatial gap in emission factors of 280.2 g kWh<sup>-1</sup> under C3 in 2030 would be 34.8% lower than the gap under C1. The difference between C3 and C1 would increase to 65.8% and 65.2% by 2045 and 2060. The narrowing in spatial gap under C3 translates to reduced differences in GHG emission intensity of PV manufacturing, and will reduce trade barriers and mobilize global trade if policies like Carbon Border Adjustment Mechanisms (CBAM) are enacted in the industry. Consequent spatial gaps in GHG emission intensities of manufacturing countries under C3 would be 42.3% lower than that under C1 by 2030. Thus, shifting from C1 to C3 translates into a decrease in GHG leakage and potential associated costs from trading PV products, especially importing from Asian countries. This rule applies for other internationally traded products as well, suggesting the additional benefits of C3 to alleviate trade barriers and give full play to the comparative advantages of countries through a globalized industrial chain.

The dynamics in the GHG emissions and mitigation can be characterized by Carbon Payback Time (CPT)<sup>39</sup>. Carbon payback time is defined as the time required to recover the GHG emitted during the manufacturing process through GHG mitigation in the power generation process. Therefore, the CPT depends on both the GHG emissions intensities during manufacturing, and the GHG mitigation intensity. Taking China, the largest manufacturing and installation country, as an example, the CPT decreases from 2.89 to 0.83 years from 2009 to 2019. The future CPT is also subject to the spatial distribution of the industry chain. In 2030, the CPT is longest (1.30 years) under M2 scenario and the shortest (0.77 year) under M3 scenario (Supplementary Table 13). Quantifying the environmental burdens of products in the future, necessitates dynamic projections of life-cycle inventory data within the context of societal, technical, and economic pathways



through prospective life-cycle assessment, particularly those related to energy-intensive activities. A promising approach emerging in this field involves integrating results from Integrated Assessment Models (IAMs) within the framework of different climate mitigation pathways. One tool that exemplifies this integration is the PRospective EnvironMental Impact asSEment (premise)<sup>40</sup> which facilitates the development of LCA databases based on prospective scenarios. Such integration with IAMs under explicit climate targets could be further integrated into future scenarios analysis to gain a deeper understanding of the potential consequences and trade-offs associated with different pathways.

Apart from GHG emissions and mitigation, the environmental impacts of the entire solar PV industry chain vary both spatially and temporally. Our results show that in China, the water consumption, primary energy demand, metal depletion, fine particulate matter formation, terrestrial acidification, human toxicity, and fossil resource scarcity intensity per functional unit decreased by 82.7%, 74.0%, 29.0%, 67.6%, 67.7%, 68.6% and 73.7% respectively, from 2009 to 2019. The cumulative amount of water consumption, primary energy demand, metal depletion, fine particulate matter formation, terrestrial acidification, human toxicity, and fossil resource scarcity intensity reached 28.00 Gt,  $12.24 \times 10^{12}$  MJ, 15.76 Mt Cu Eq, 1023.3 kt PM<sub>2.5</sub> Eq, 2715.2 kt SO<sub>2</sub> Eq, 3218.4 Mt 1,4-DCB, 205.7 Mt oil Eq during this period (Supplementary Table 14). In the future, the environmental indicators will be subject to the spatial distribution of the industrial chain, especially the manufacturing patterns (Supplementary Table 15 and Supplementary Methods). Water consumption, energy demand, human toxicity and fossil resource scarcity are more sensitive to the spatial pattern compared to metal depletion, fine particulate matter formation, and terrestrial acidification. Our results show that, on average, M2 scenarios increased the water consumption, energy demand, human toxicity and fossil resource scarcity by 26.0%, 15.0%, 7.1% and 15.3%, respectively, by 2060 compared to M3. Therefore, special attention needs to be paid to environmental impacts that are particularly sensitive to the deployment of the industrial chain. Furthermore, the land use occupied by installed stations was estimated to be at most 7288.0 km<sup>2</sup> by 2019, and it is projected to reach between 85–202 thousand km<sup>2</sup> by 2060, with C1 and C3 installations occupying less land due to their priority for installation in countries with lower latitudes and higher land occupation ratios (Supplementary Table 15 and Supplementary Methods).

## Discussion

The study reveals the spatial and temporal evolution of the emission and mitigation intensities of the solar PV industrial chain, applying spatiotemporal data to take account of historical net GHG savings. As the study suggests, the differing spatial and temporal characteristics of the mitigation and emission intensities prove detrimental to realistic accounting of GHG emissions and mitigation. Thus, the future spatiotemporal evolution of the emission and mitigation intensities are projected and integrated in the comparison of net savings in GHG emissions under nine scenarios. The feedback effects of solar power installation on the mitigation and emission intensity of solar power are dynamically modeled. Combining with nine manufacturing and installation scenarios, the study projects the spatially dynamic trajectories of emissions and mitigation and offers guidance for global decarbonization through increased cooperative international development of the solar PV industrial chain.

Based on analysis of evolving differences in mitigation intensity, the results indicate evident differences in the total amount

and contributors of future GHG mitigation under three installation scenarios. If the installation pattern is targeted to exploit comparative advantages in GHG mitigation intensities among nations (C3), the global GHG mitigation would increase by 92.1 Gt CO<sub>2</sub>e compared to a scenario locking in current patterns (C1), 1.8 times global GHG emissions from all sources in 2020. Such increased GHG mitigation with the same amount of global total PV capacity could be achieved by seizing opportunities reflected by the differences in GHG mitigation, and dynamically adjusting the installation priority based on the evolution of mitigation intensity according to solar installation dynamics and ongoing decarbonization status of the power system. Although the analysis is conducted at a global scale, the findings have general implications for regional and national practices. When developing the strategy of substitution of low-carbon technologies for traditional carbon-intensive ones, optimizing the distribution to take account of both the scalability and potential of low-carbon technologies and the emission characteristics of existing ones could achieve better GHG mitigation without increasing total investment.

The targeted deployment of solar PV of the C3 scenario increases the capacity for the Africa, Eurasia, the Middle East, and ASEAN regions by 1.1 TW, 1.3 TW, 1.3 TW and 1.5 TW compared to C1 (Fig. 6g, h, Supplementary Figure 8). In addition to enhanced GHG mitigation, targeted deployment in these regions would bring extensive co-benefits, including but not limited to enabling affordable and clean power supply for people without electricity access; accelerating clean energy substitution of manufacturing sectors; reducing air pollution and associated health damage, together serving Sustainable Development Goals (SDGs)<sup>41</sup>. An estimated 757 million people live without electricity access in 2020, of which 77.2% and 17.6% are in Africa and Asia respectively<sup>42</sup>. Furthermore, countries in Asia, Africa, and the Middle East have the highest levels of ambient fine particle pollution, with the 10 countries with the highest PM<sub>2.5</sub> exposures in these regions<sup>43</sup>. To better realize these co-benefits of GHG mitigation would require effective international coordination to overcome lagging deployment in these regions. Developed countries could assist developing countries with high GHG mitigation intensities through finance and technical support in solar power development, exploiting comparative advantages in GHG mitigation to offset domestic GHG emissions. Furthermore, international climate funds for renewable energy could flow to countries with the highest GHG mitigation potentials to accelerate progress in global decarbonization. It is important to note that the deployment of PV in resource-rich or less-favorable locations within a country could lead to different capacity factors and increase variance in the mitigation value of deploying PV<sup>36</sup>. Our study aimed to compare deployment strategies across countries from a global perspective. However, due to the difficulty in factoring in numerous natural and social factors that influence siting decisions<sup>44</sup>, we used nationally averaged resources and power grid condition parameters and did not account for spatial variation within a country. Nonetheless, by utilizing national average conditions, our study provides valuable insights into deployment strategies that can inform global energy policies. Future studies could pay special attention to the impact of deployment pathways within a country, especially for countries with large intra-country differences.

The assumption that solar power will substitute the average grid power is a simplification that may not hold in the real world. The substituted power source will depend on the season, time of day, and will vary with solar penetration levels<sup>45</sup>. For instance, the substituted power may differ from those used during nighttime, given the typical diurnal fluctuations of PV output. To account for this complexity, we took the average emissions factor of the power grid as an approximation of the emissions factor of the

offset power sources. However, additional efforts are necessary to examine the substituted power source of solar PV after disaggregating the intertwined factors, especially considering the impact of efforts to better match solar supply with demand in future power systems, such as load management and pairing solar with storage<sup>4,46</sup>. Paired storage facilities are expected to improve the variability of solar power with higher penetration of solar power in the grid<sup>47</sup>. However, assuming chemistry energy storage is paired with solar power from 2030 onwards<sup>48,49</sup>, and taking into account the observed modeling results that demonstrate a non-linear increase in storage capacity with the share of solar power in the power mix<sup>50</sup>, cumulative GHG emissions from energy storage systems could range from 5.2–7.1 Gt by 2060 (lithium-ion batteries) and 5.9–8.2 Gt (vanadium redox flow batteries) (Supplementary Table 16 and Supplementary Methods). Water consumption, primary energy demand, metal depletion, fine particulate matter formation, terrestrial acidification, human toxicity, and fossil resource scarcity of energy storage systems range from 0.2–0.4 times, 0.7–1.3 times, 0.8–1.2 times, 0.2–0.3 times, 0.1–0.3 times, 0.1–0.2 times and 0.4–0.6 times that of the entire solar PV industry during the same period (Supplementary Table 16). This indicates that further efforts are needed to reduce the environmental impacts of paired storage to truly convert solar PV into clean energy. Additionally, such incorporation of storage will increase the PV investment by 9.4–33.1%, depending on the future cost and installation scenarios (Supplementary Table 16). While the study provided an approximate estimation of the environmental burden associated with storage capacities, it is important to note that the exact storage capacity required for pairing with solar power needs to consider the specific power configuration of other components within the power system. This includes considerations such as the composition of the overall power supply mix, the presence of other flexibility enablers like demand-side management, and the technical and economic constraints inherent in power grid dispatch operations. These factors play a crucial role in determining the optimal storage capacity needed for effective integration of solar power into the grid.

At a time when the international industrial supply chain of PV has gained increased attention, the results of this study are particularly helpful from the perspective of manufacturing. It illustrates diverse emission trajectories under differing global manufacturing pathways. Although PV manufacturing emissions are generally dwarfed by those mitigated through solar displacement of thermal generation, the differences in emission intensities draws attention to the elevated cost of PV installation in a volatile international environment. If manufacturing were to follow recent examples, by relocating to Asia-Pacific regions outside of China (M2) to leverage better trade conditions and low-cost labor, the emissions by 2060 could be 42.9% and 91.7% higher than the pathways further concentrating the supply chain in China (M1) or moving it to the Europe and North America (M3). If this difference in emissions from importing PV products (Supplementary Table 17) were charged at \$75 ton<sup>-1</sup> CO<sub>2</sub> in the US and European Union (through policies like CBAM<sup>51</sup>) and 50% of such fees were borne by the PV installers, then importing products from Asia (M2) would additionally cost installers \$6.0–9.8 per kW, equivalent to 3.5–5.8% of estimated module cost in 2030<sup>52</sup>. Thus, reducing or exempting such fees for PV and other GHG mitigation technologies could reduce domestic GHG mitigation costs. Beyond the elevated mitigation cost, the shift of manufacturing locations may lead to mismatches between the supply and demand of key resource materials such as the metals like silver and tellurium required for photovoltaic modules<sup>53</sup>. If these raw materials were to be redistributed through international trade, the complex international situation may lead to

fluctuations in product prices and potential risks to the stable supply of PV products. Anticipating and responding to environmental risks arising from such a shifting geographical pattern of PV manufacturing will benefit from a comprehensive early assessment.

## Methods

**Life-cycle assessment framework.** A life cycle assessment (LCA) method is employed to calculate the cradle-to-cradle GHG emissions of solar photovoltaic power generation worldwide. The product in this analysis is crystalline silicon PV power generation systems, including those employing monocrystalline silicon and polysilicon technologies. GHG emissions are assessed based on the 100-year Global Warming Potential (GWP), expressed in kg CO<sub>2</sub> equivalent (kg CO<sub>2</sub>e) following the methods of CML 2001 (January 2016) developed at Leiden University<sup>54</sup>. The assessment unit is a 1 kW solar PV power generation system, capable of generating 1 kWh of electricity per hour under standard test conditions (module temperature, 25 °C; air mass, 1.5 standard spectrum; solar irradiance, 1 kW m<sup>-2</sup>). Following common practice<sup>14,55</sup>, the generation system boundary in this study includes the following steps: production of metallurgical polysilicon, solar grade polysilicon, silicon ingots, wafers, cells, modules, and other components to make the power generation system work (balance of system); assembly, operational use, and eventual disposal and recycling of the generation system; and transportation of intermediate and final products and recycled materials (Supplementary Methods). The silicon ore mining process has been excluded from the system boundary because of its negligible GHG emissions compared to the rest of the processes<sup>11,19</sup>. See Supplementary Figure 4 for detailed information and Supplementary Table 18 for inputs and emission inventories for each step. The base life-cycle inventory (LCI) refer to the baseline life-cycle inventory released by IEA-PVPS Task 12<sup>56</sup>, which represents the average inputs, outputs, and emissions of manufacturing processes for crystalline silicon-based supply chain products, as well as supplemental information collected from the published research literature<sup>13,20,22</sup>. The LCA was performed using GaBi Version 10.6.1.35 and supported by the GaBi database version 2023.1. The research dynamically characterizes technical parameters regarding the intensities of electricity and steam use in each process; silicon use efficiency in wafer slicing; and solar-to-power conversion efficiency<sup>57–62</sup>. The specific settings of all technical parameters are illustrated in the Supplementary Methods. The emissions in our study have been spatialized to account for variations among different countries<sup>63</sup>. This spatialization takes into consideration the specific power emissions factors associated with each country, as well as the dynamic power consumption patterns observed during different steps of the analysis.

**GHG emissions and mitigation.** The annual GHG emissions in each step are estimated based on the emission intensity and the activity levels of the subject countries<sup>64,65</sup>. The historical manufacturing data for each step are adopted from the annual report on PV application trends issued by the IEA<sup>8</sup>.

The annual global GHG emissions of the industry are calculated with the equation:

$$E_t = \sum_{s=1}^9 \sum_{i=1}^{si} P_{s,i,t} \cdot EI_{i,t,s} \quad (1)$$

where  $E_t$  indicates the GHG emissions in year  $t$ ;  $s$  is a step code, with 1 to 9 representing production of metallurgical grade silicon, solar-grade polysilicon, silicon ingots, wafers, solar cells, module, and BOS; assembly and operations; and disposal/recycling of the

system;  $i$  is an index for countries involved in step  $s$  and  $si$  the total number of such countries;  $P_{s,i,t}$  indicates the activity level in step  $s$  of country  $i$  in year  $t$ ; and  $EF_{i,t,s}$  indicates the GHG emission intensity for country  $i$  in year  $t$  in step  $s$ .

The historical GHG mitigation of the installed PV capacity is evaluated based on the total installed capacity, capacity factor, and power system emission factors.

$$A_t = \sum_{i=1}^{ai} EF_{i,t} \cdot CP_{i,t} \cdot CF_{i,t} \cdot 8760 \quad (2)$$

where the  $A_t$  indicates the GHG mitigation in year  $t$ ;  $i$  is an index for countries involved in installation of solar PV and  $ai$  is the number of such countries;  $EF_{i,t}$  is the system-wide average GHG emission factor for power generation in country  $i$  in year  $t$ ;  $CP_{i,t}$  is the PV installed capacity for country  $i$  in year  $t$ ; and  $CF_{i,t}$  is the average PV capacity factor of country  $i$  in year  $t$ . The capacity factor for each country is calculated according to the methods described by Lu et al.<sup>4</sup>, and the installed capacity data are adopted from the WIND database<sup>66</sup>.

The net GHG mitigation  $NA_t$  is defined as the difference between GHG mitigation and GHG emissions as defined above:

$$NA_t = A_t - E_t \quad (3)$$

For future projections of GHG mitigation, the mitigation effects are not only reflected in the substitution of grid power but also the PV impact on grid emission factors, especially for the scenario where solar power installation is prioritized for regions with higher power generation GHG emission factors. Therefore, here we calculate a base scenario in which solar installed capacity remains at the level of 2019 and other conditions remain unchanged, and define the entire power system emissions avoided relative to this base scenario as the future GHG mitigation.

$$A_t = \sum_{i=1}^{ai} (EF_{i,t} \cdot PD_{i,t} - EFB_{i,t} \cdot PD_{i,t}) \quad (4)$$

where the  $PD_{i,t}$  indicates the power demand for country  $i$  in year  $t$ ; and  $EFB_{i,t}$  is the system-wide average GHG emission factor for power generation in country  $i$  in year  $t$  under the base scenario. The calculation is introduced in the following section.

**GHG emission factor of the power grid.** The GHG emission factor of the power grid is the primary determinant of GHG mitigation intensity of solar PV substitution as well as the GHG emission intensities during manufacturing processes<sup>67</sup>. The historical emissions factor is derived from IEA (Supplementary Table 19). The utilization of the IEA grid emission factor in this study may result in a potential slight underestimation of the true emissions and mitigation associated with the PV industry chain. This limitation arises from the fact that the IEA grid emission factor does not encompass the entirety of emissions across the life cycle perspective. The GHG emissions factor of the power system for country  $i$  in future year  $t$  is expressed in the following equation:

$$EF_{pg,i,t} = EF_{npv,i,t} \times S_{npv,i,t} + EF_{pv,i,t} \times S_{pv,i,t} \quad (5)$$

where  $EF_{npv,i,t}$  represents the average emission factor of all power sources in the grid other than solar PV and  $EF_{pv,i,t}$  is the emission factor for PV, in both cases for country  $i$  in year  $t$ , and to maintain consistency with the IEA emission factor, the PV emission factor is set as zero based on the logic of fossil fuel usage during power generation process; and  $S_{npv,i,t}$  and  $S_{pv,i,t}$  represent the power generation shares of other power sources and solar PV in the system.

The change in  $EF_{npv,i,t}$  over time is assumed to reflect the strength of a country's carbon neutrality target (Supplementary

Table 7). The study considers three scenarios to project the path of future decarbonization of other power sources in the grid. Under optimistic, modest, and conservative scenarios, it is assumed that for countries with carbon neutrality targets, the  $EF_{npv,i,t}$  is assumed to reach net-zero 10, 5, and 0 years earlier than those targets, based on a common expectation that decarbonization of the power sector must precede that of other sectors, given that many of them will be decarbonized through electrification. As for countries without carbon neutrality targets, it is assumed that the average emission factor of non-solar power sources will decrease by 1%, 0.5%, and 0.1% of the base level from 2019 annually under the optimistic, modest, and conservative scenarios.

$S_{pv,i,t}$  is related to the installed capacity of solar power and can be expressed with the following equation:

$$S_{pv,i,t} = E_{pv,i,t} / PD_{i,t} \quad (6)$$

where  $E_{pv,i,t}$  refers to the annual power generation of solar PV and  $PD_{i,t}$  is power demand as defined for Eq. (4), and the international power trade is not considered in the study. The  $EF_{pv,i,t}$  is set to zero to simplify the calculation given its negligible value in practice<sup>68,69</sup>. The national power demand is obtained through down-scaling the regional power demand reported by IEA<sup>70</sup>. Each country is weighted by a composite factor determined by population and GDP, noting that the power demand historically is strongly related to the GDP per capita ( $GDP_{i,t}$ ) and population ( $POP_{i,t}$ ). Here the composite factor is estimated by extrapolating an empirical curve fitting the historical global national power generation to  $GDP_{i,t}$  and  $POP_{i,t}$  from 1995 to 2015<sup>71</sup>. Future GDP and population projections are derived from the Shared Socioeconomic Pathways 1 (SSP1)<sup>72</sup>, which suggests a sustainable future with low challenges both for mitigation and adaption for climate change. The  $E_{pv,i,t}$  depends on the installation pathways as introduced in the next section and is calculated as follows:

$$E_{pv,i,t} = CP_{i,t} \cdot CF_{i,t} \cdot 8760 \quad (7)$$

where other variables are defined as above for Eq. (2).

**Installation and manufacturing pathways.** The study sets up three installation scenarios to investigate the impact of the deployment pattern on GHG mitigation, with results summarized by nation/region in Supplementary Figure 8. The first scenario (C1) locks in the current pattern of installation, with the share of newly installed solar power generation to meet each nation's power demand ( $SS_{i,t}$ ) proportional to the share of solar for power demand in 2019 ( $S_{p,19}$ ) (Eq. 8). The second scenario (C2) is based on a principle of  $SS_{i,t}$ -based equity for new installation, with the same  $SS_{i,t}$  projected for all nations in the same year.

$$SS_{i,t} \propto S_{i,19}(M1) \quad (8)$$

The newly installed capacity of nation  $i$  in year  $t$  ( $NC_{i,t}$ ) is derived based on the above assumptions in each scenario and shared assumption about the growth trajectory for the global installed capacity of solar PV ( $CP_t$ ) (Eqs. 9–11):

$$SS_{i,t} = \frac{NC_{i,t} * CF_{i,t} * 8760}{PD_{i,t}} \quad (9)$$

$$\sum_{i=1}^{185} CP_{i,t} = CP_t \quad (10)$$

$$SCP_{i,t} = \frac{CP_{i,t} * CF_{i,t} * 8760}{PD_{i,t}} \quad (11)$$

where  $SS_{i,t}$  denotes the share of newly installed solar power

generation to meet power demand of nation  $i$  in year  $t$ . In addition, the study assumes that the maximum solar power share in the power supply is 70%, referring to the simulated share of solar power in total electricity generation with 100% wind, solar and hydro supply for various countries<sup>35</sup> whilst also considering the limits of the grid to integrate intermittent solar power, as it challenges many aspects of grid operation including flexibility, voltage, and frequency<sup>1,73,74</sup>. In addition, the installed capacity of solar power in each country is set to not exceed the national technical solar potential considering geographical and meteorological constraints<sup>4</sup>. For any nation  $i$  in any year  $t$ , if the optimized power generation from solar PV equals or exceeds 70% of the power demand ( $SCP_{i,t} \geq 70\%$ ), or the installed capacity exceeds the technical potential, the  $CP_{i,t}$  is set to the smaller theoretical maximum, according to the above criteria, and any unrealized newly installed capacity is allocated to other nations based on the same allocation criteria.

The third scenario (C3) seeks to take the marginal GHG mitigation intensity into account in the deployment pattern, dynamically prioritizing new capacity installations in nations with the highest average GHG emission factors in their power systems. This is accomplished using an iterative calculation, with the amount of newly installed solar PV capacity in each modeling iteration allocated according to the following criteria: new capacity is allocated to the nation with the highest GHG mitigation intensity, subject to the aforementioned constraints of a 70% maximum solar share of power generation and the nation's maximum solar PV potential; if one of the constraints is binding, additional new capacity is allocated to the country with the next highest grid GHG emission factor, subject to the same constraints; iterations continue until all new installations required globally for the given year are allocated. For each iteration, the model updates the GHG emission factors after quantifying the impact of the new solar installations.

The study includes three manufacturing scenarios (Supplementary Table 6). The common assumption is that new distributions are established by 2030 and they are held constant at 2030 levels. The first (M1) assumes continued concentration in China based on past trends, projecting that 90% of the production for each process would continue to occur in China in and after 2030 and the remaining 10% of production would occur according to the current (2019) national shares, scaling linearly over time to reflect supply growth. The second (M2) assumes major transfer of manufacturing to Asia-Pacific countries outside of China, referring to recent industrial cases taking advantage of low manufacturing costs and a relatively open international trade environment<sup>11</sup>. It assumes that 90% of production of each process will occur in Asia-Pacific countries in and after 2030 (assuming equal distribution in India, Vietnam, Malaysia, South Korea and the Philippines)<sup>11</sup> and the remaining 10% as in M1, with both varying linearly. The last manufacturing scenario (M3) assumes mass transfer of manufacturing to major countries in the Europe and North America, with the top 5 countries in PV installations (who are also largest regional manufacturers) in 2019 (United States, Germany, Italy, France, and Spain), linearly increasing their shares of manufacturing of all intermediate and final PV products to 18% in and after 2030, together accounting for 90%; with the remaining 10% as in M1 and again with linear scaling over the modeling time period.

#### Data availability

Data that support the findings of this study are available at <https://doi.org/10.5281/zenodo.8275019>.

#### Code availability

Code used for this analysis is available at <https://doi.org/10.5281/zenodo.8275019>.

Received: 30 January 2023; Accepted: 15 September 2023;

Published online: 11 October 2023

#### References

- International renewable energy agency. Future of solar photovoltaic. (IRENA, Abu Dhabi, 2019).
- McCollum, D. L. et al. Energy investment needs for fulfilling the Paris Agreement and achieving the sustainable development goals. *Nat. Energ.* **3**, 589–599 (2018).
- Victoria, M. et al. Solar photovoltaics is ready to power a sustainable future. *Joule* **5**, 1041–1056 (2021).
- Lu, X. et al. Combined solar power and storage as cost-competitive and grid-compatible supply for China's future carbon-neutral electricity system. *Proceedings of the National Academy of Sciences of the United States of America* **118**, <https://doi.org/10.1073/pnas.2103471118> (2021).
- Energy and Climate Intelligence Unit. Race to Net Zero: Carbon Neutral Goals by Country.
- Haegel, N. M. et al. Terawatt-scale photovoltaics: transform global energy. *Science* **364**, 836 (2019).
- International energy agency. Net zero by 2050: A roadmap for the global energy sector. (2021).
- International energy agency. Trends in PV applications 2019. (2020).
- International energy agency. Trends in PV applications 2016. (2017).
- Binz, C., Tang, T. & Huenteler, J. Spatial lifecycles of cleantech industries – The global development history of solar photovoltaics. *Energy Policy* **101**, 386–402 (2017).
- International energy agency. Special report on solar PV global supply chains. (2022).
- Congress of USA. Solar energy manufacturing for America act. (2021).
- Fu, Y., Liu, X. & Yuan, Z. Life-cycle assessment of multi-crystalline photovoltaic (PV) systems in China. *J. Clean. Prod.* **86**, 180–190 (2015).
- Hong, J., Chen, W., Qi, C., Ye, L. & Xu, C. Life cycle assessment of multicrystalline silicon photovoltaic cell production in China. *Sol. Energy* **133**, 283–293 (2016).
- Ludin, N. A. et al. Prospects of life cycle assessment of renewable energy from solar photovoltaic technologies: A review. *Renew. Sust. Energ. Rev.* **96**, 11–28 (2018).
- Muteri, V. et al. Review on life cycle assessment of solar photovoltaic panels. *Energies* **13**, <https://doi.org/10.3390/en13010252> (2020).
- Pu, Y. et al. Environmental effects evaluation of photovoltaic power industry in China on life cycle assessment. *Journal of Cleaner Production* **278**, <https://doi.org/10.1016/j.jclepro.2020.123993> (2021).
- Xie, M. et al. Pollutant payback time and environmental impact of Chinese multi-crystalline photovoltaic production based on life cycle assessment. *J. Clean. Prod.* **184**, 648–659 (2018).
- Yang, D., Liu, J., Yang, J. & Ding, N. Life-cycle assessment of China's multi-crystalline silicon photovoltaic modules considering international trade. *J. Clean. Prod.* **94**, 35–45 (2015).
- Huang, B. et al. Environmental influence assessment of China's multi-crystalline silicon (multi-Si) photovoltaic modules considering recycling process. *Sol. Energy* **143**, 132–141 (2017).
- Louwen, A., van Sark, W. G., Faaij, A. P. & Schropp, R. E. Re-assessment of net energy production and greenhouse gas emissions avoidance after 40 years of photovoltaics development. *Nat. Commun.* **7**, 13728 (2016).
- Xu, L., Zhang, S., Yang, M., Li, W. & Xu, J. Environmental effects of China's solar photovoltaic industry during 2011–2016: A life cycle assessment approach. *J. Clean. Prod.* **170**, 310–329 (2018).
- Wang, M. et al. Breaking down barriers on PV trade will facilitate global carbon mitigation. *Nat. Commun.* **12**, 6820 (2021).
- Wikoff, H. M., Reese, S. B. & Reese, M. O. Embodied energy and carbon from the manufacture of cadmium telluride and silicon photovoltaics. *Joule* **6**, 1710–1725 (2022).
- International Energy Agency. Snapshot of Global PV Markets 2021. (2021).
- International Energy Agency. Global energy review 2019. (2020).
- Bensch, G., Jeuland, M. & Peters, J. Efficient biomass cooking in Africa for climate change mitigation and development. *One Earth* **4**, 879–890 (2021).
- Li, H., Ai, X., Wang, L. & Zhang, R. Substitution strategies for cooking energy: To use gas or electricity? *J. Environ. Manage.* **303**, 114135 (2022).
- Wang, S. et al. Drivers of CO<sub>2</sub> emissions from power generation in China based on modified structural decomposition analysis. *J. Clean. Prod.* **220**, 1143–1155 (2019).
- Yan, Q., Wang, Y., Balezenti, T. & Streimikiene, D. Analysis of China's regional thermal electricity generation and CO<sub>2</sub> emissions: Decomposition based on the generalized Divisia index. *Sci. Total Environ.* **682**, 737–755 (2019).

31. Fondazione Eni Enrico Mattei (FEEM). Towards the decarbonization of the power sector – a comparison of China, the EU and the US based on historical data. (2021).
32. Momodu, A. S., Okunade, I. D. & Adepoju, T. D. Decarbonising the electric power sectors in sub-Saharan Africa as a climate action: A systematic review. *Environmental Challenges* 7, <https://doi.org/10.1016/j.envc.2022.100485> (2022).
33. Kommalapati, R., Kadiyala, A., Shahriar, M. & Huque, Z. Review of the life cycle greenhouse gas emissions from different photovoltaic and concentrating solar power electricity generation systems. *Energies* 10, <https://doi.org/10.3390/en10030350> (2017).
34. Lunardi, M. M., Dias, P. R., Deng, R. & Corkish, R. in *Photovoltaic Sustainability and Management* 1–34 (2021).
35. Jacobson, M. Z. et al. Low-cost solutions to global warming, air pollution, and energy insecurity for 145 countries. *Energy Environ. Sci.* 15, 3343–3359 (2022).
36. Chen, S. et al. The potential of photovoltaics to power the belt and road initiative. *Joule* 3, 1895–1912 (2019).
37. Chowdhury, M. S. et al. An overview of solar photovoltaic panels' end-of-life material recycling. *Energy Strategy Reviews* 27, <https://doi.org/10.1016/j.esr.2019.100431> (2020).
38. Mehedi, T. H., Gemechu, E. & Kumar, A. Life cycle greenhouse gas emissions and energy footprints of utility-scale solar energy systems. *Appl. Energy* 314, 118918 (2022).
39. Tsang, M. P., Sonnemann, G. W. & Bassani, D. M. Life-cycle assessment of cradle-to-grave opportunities and environmental impacts of organic photovoltaic solar panels compared to conventional technologies. *Sol. Energy Mater. Sol. Cells* 156, 37–48 (2016).
40. Sacchi, R. et al. Prospective environmental impact assessment (premise): A streamlined approach to producing databases for prospective life cycle assessment using integrated assessment models. *Renewable and Sustainable Energy Reviews* 160, <https://doi.org/10.1016/j.rser.2022.112311> (2022).
41. Moner-Girona, M., Kakoulaki, G., Falchetta, G., Weiss, D. J. & Taylor, N. Achieving universal electrification of rural healthcare facilities in sub-Saharan Africa with decentralized renewable energy technologies. *Joule* 5, 2687–2714 (2021).
42. International energy agency. Access to electricity. (2020).
43. The Health effects institute and the institute for health metrics and evaluation. State of global air 2020. (2020).
44. Wang, C.-N., Dang, T.-T., Nguyen, N.-A.-T. & Wang, J.-W. A combined Data Envelopment Analysis (DEA) and Grey Based Multiple Criteria Decision Making (G-MCDM) for solar PV power plants site selection: A case study in Vietnam. *Energy. Rep.* 8, 1124–1142 (2022).
45. Heptonstall, P. J. & Gross, R. J. K. A systematic review of the costs and impacts of integrating variable renewables into power grids. *Nat. Energy* 6, 72–83 (2020).
46. Jordehi, A. R. Optimisation of demand response in electric power systems, a review. *Renew. Sust. Energy. Rev.* 103, 308–319 (2019).
47. Ershad, A. M., Ueckerdt, F., Pietzcker, R. C., Giannousakis, A. & Luderer, G. A further decline in battery storage costs can pave the way for a solar PV-dominated Indian power system. *Renewable and Sustainable Energy Transition* 1, <https://doi.org/10.1016/j.rset.2021.100006> (2021).
48. da Silva Lima, L. et al. Life cycle assessment of lithium-ion batteries and vanadium redox flow batteries-based renewable energy storage systems. *Sustainable Energy Technologies and Assessments* 46, <https://doi.org/10.1016/j.seta.2021.101286> (2021).
49. Han, X. et al. Comparative life cycle greenhouse gas emissions assessment of battery energy storage technologies for grid applications. *Journal of Cleaner Production* 392, <https://doi.org/10.1016/j.jclepro.2023.136251> (2023).
50. Rauegi, M., Leccisi, E. & Pthenakis, V. M. What Are the Energy and Environmental Impacts of Adding Battery Storage to Photovoltaics? A Generalized Life Cycle Assessment. *Energy Technology* 8, <https://doi.org/10.1002/ente.201901146> (2020).
51. Parry, I., Black, S. & Roaf, J. Proposal for an International Carbon Price Floor among Large Emitters. (International Monetary Fund, 2021).
52. Solar Energy Technologies Office. 2030 Solar Cost Targets. (US Department of Energy, 2021).
53. Carrara, S., Alves Dias, P., Plazzotta, B. and Pavel, C. Raw materials demand for wind and solar PV technologies in the transition towards a decarbonised energy system. (2020).
54. CML-Department of Industrial Ecology. CML-IA Characterisation Factors. (2016).
55. Müller, A. et al. A comparative life cycle assessment of silicon PV modules: Impact of module design, manufacturing location and inventory. *Solar Energy Materials and Solar Cells* 230, <https://doi.org/10.1016/j.solmat.2021.111277> (2021).
56. The international Energy Agency. Life cycle inventories and life cycle assessments of photovoltaic systems 2020. (2020).
57. China Photovoltaic Industry Association. Annual report of China's photovoltaic industry. (2009–2020).
58. Yu, Z. *Study on life cycle assessment of metallurgical polysilicon and grid-connected photovoltaic system*, Kunming University of Science and Technology, (2017).
59. Li, Y. *Life cycle assessment of crystalline silicon modules in China* Master thesis, Shanghai Jiao Tong University, (2015).
60. He, Y. *Life cycle assessment of solar grade polysilicon*, Southwest Jiaotong University, (2013).
61. He, J. *Research on carbon emission of photovoltaic power generation based on life cycle assessment*, Nanjing University of Aeronautics and Astronautics, (2017).
62. Liang, J. *Research on the life cycle environmental impact of building grid-connected photovoltaic system*, Tianjin University, (2012).
63. Chen, S. et al. in *Data for 'Deploying PV first in carbon-intensive regions brings gigatons more carbon mitigations to 2060'* (<https://doi.org/10.5281/zenodo.8275019>, 2023).
64. IEA PVPS. Trends in photovoltaic applications. (2009–2020).
65. Chen, S. et al. in *Data for 'Deploying PV first in carbon-intensive regions brings gigatons more carbon mitigations to 2060'* (<https://doi.org/10.5281/zenodo.8275071>, 2023).
66. WIND database. Global installed capacity of solar PV power generation. (2020).
67. Liu, F. & van den Bergh, J. C. J. M. Differences in CO2 emissions of solar PV production among technologies and regions: Application to China, EU and USA. *Energy Policy* 138, <https://doi.org/10.1016/j.enpol.2019.111234> (2020).
68. International energy agency. Emissions factors 2020. (2020).
69. Hertwich, E. G. et al. Integrated life-cycle assessment of electricity-supply scenarios confirms global environmental benefit of low-carbon technologies. *Proc. Natl. Acad. Sci. USA* 112, 6277–6282, <https://doi.org/10.1073/pnas.1312753111> (2015).
70. International energy agency. World energy Outlook 2021. (2022).
71. World Bank. World Development Indicators. (2022).
72. O'Neill, B. C. et al. The roads ahead: Narratives for shared socioeconomic pathways describing world futures in the 21st century. *Global Environmental Change* 42, 169–180, <https://doi.org/10.1016/j.gloenvcha.2015.01.004> (2017).
73. Gandhi, O., Kumar, D. S., Rodríguez-Gallegos, C. D. & Srinivasan, D. Review of power system impacts at high PV penetration Part I: Factors limiting PV penetration. *Solar Energy* 210, 181–201, <https://doi.org/10.1016/j.solener.2020.06.097> (2020).
74. International Energy Agency. World Energy Outlook 2022. (2022).

## Acknowledgements

This work was supported by National Natural Science Foundation of China (72025401, 71974108, 72140003, and 72204132), the China Postdoctoral Science Foundation BX2021148, the Shuimu Tsinghua Scholar Program 2021SM014, the Tsinghua University-Inditex Sustainable Development Fund, the Ordos-Tsinghua Innovative & Collaborative Research Program in Carbon Neutrality, the Tsinghua-Toyota Joint Research Institute Cross-discipline Program, and Office of the President of Harvard University and the Harvard Global Institute grants to the Harvard-China Project on Energy, Economy, and Environment. We thank technical experts from LONGi for technical consultation, and the reviewers for key insights and comments.

## Author contributions

Shi Chen: conceptualization, methodology, data curation, formal analysis, writing – original draft, writing – review & editing, funding acquisition. Xi Lu: supervision, funding acquisition, conceptualization, formal analysis, writing – review & editing. Chris P. Nielsen: writing – review & editing. Michael B. McElroy: supervision, writing – review & editing. Gang He: writing – review & editing. Shaohui Zhang: writing – review & editing. Kebin He: writing – review & editing. Xiu Yang: writing – review & editing. Fang Zhang: writing – review & editing. Jiming Hao: supervision, writing – review & editing.

## Competing interests

The authors declare no competing interests.

## Additional information

**Supplementary information** The online version contains supplementary material available at <https://doi.org/10.1038/s43247-023-01006-x>.

**Correspondence** and requests for materials should be addressed to Xi Lu or Michael B. McElroy.

**Peer review information** *Communications Earth & Environment* thanks Christian Bauer, Hanna Breunig and the other, anonymous, reviewer(s) for their contribution to the peer review of this work. Primary Handling Editors: Sagar Parajuli, Joe Aslin and Clare Davis. A peer review file is available.

**Reprints and permission information** is available at <http://www.nature.com/reprints>

**Publisher's note** Springer Nature remains neutral with regard to jurisdictional claims in published maps and institutional affiliations.



**Open Access** This article is licensed under a Creative Commons Attribution 4.0 International License, which permits use, sharing, adaptation, distribution and reproduction in any medium or format, as long as you give appropriate credit to the original author(s) and the source, provide a link to the Creative Commons license, and indicate if changes were made. The images or other third party material in this article are included in the article's Creative Commons license, unless indicated otherwise in a credit line to the material. If material is not included in the article's Creative Commons license and your intended use is not permitted by statutory regulation or exceeds the permitted use, you will need to obtain permission directly from the copyright holder. To view a copy of this license, visit <http://creativecommons.org/licenses/by/4.0/>.

© The Author(s) 2023